Improvement of the photo-Fenton process at natural condition of pH using organic fertilizers mixtures: potential application to agricultural reuse of wastewater

N. López-Vinent*, A. Cruz-Alcalde, J. Giménez, S. Esplugas, C. Sans

Department of Chemical Engineering and Analytical Chemistry, Faculty of Chemistry, Universitat de Barcelona, C/Martí i Franqués 1, 08028 - Barcelona, Spain. Tel: +34934021293. Fax: +34934021291

*Corresponding Author: nuria.lopez@ub.edu

ABSTRACT

Five organic fertilizers (DTPA, EDDHA, HEDTA, EDTA and EDDS) were studied as iron sources for photo-Fenton process at natural pH to remove micropollutants (MPs) from wastewater for its reuse in irrigation. The results demonstrated that the stability constant of iron chelates is a key parameter for optimal micropollutants removal and it is linked to the structure of chelator. Mixtures of organic fertilizers were also tested to overcome excessive iron loose and to optimize MPs abatement kinetics. An improvement of photo-Fenton process occurred when using chelating mixtures. For instance, with 50%EDDS + 50%EDTA total removal of propranolol (PROP) was achieved at 30 minutes while EDTA needed up to 90 min of reaction and with EDDS total degradation was not achieved. In addition, the availability of dissolved iron of the mixture at the end of the treatment was 5.5 times higher than EDDS, increasing its suitability as reuse water for irrigation.

KEYWORDS

Organic fertilizers, Wastewater reuse, Iron chelates mixtures, Photo-Fenton

1. Introduction

Water scarcity is a growing environmental problem that the world's population must confront. According to the World Wildlife Fund (WWF) and UNESCO (The United Nations Educational, Scientific and Cultural Organization), a large part of the aquatic ecosystems has changed into a stress situation during the last decades [1]. Under the current water consumption pattern, moreover, these organizations have estimated that two-thirds of the world population could suffer from water shortages by 2025 [2]. In front of this critical scenario, the reuse of wastewater (WW) is expected to be necessary to ensure the coverage of the water demand in a near future.

The water destined to agriculture is around 70% of the total freshwater demand and this percentage accounts for 90% in some developing countries. Thus, different measures are required to address the acute water challenges in agriculture for the next few years [2]. In this sense, the WW reuse in agriculture seems a good strategy to reduce the percentage of fresh water destined to this sector. However, the quality of this reclaimed WW has to accomplish some minimum requirements to ensure a safe use of this alternative resource in crop irrigation. These requisites are currently established in the Proposal for a Regulation of the European Parliament and of the Council on minimum requirements for water reuse [3], where Biochemical Oxygen Demand (BOD), turbidity and pathogens are defined as the main parameters to be controlled. Nevertheless, wastewater can also contain micropollutants (MPs), which are not completely regulated yet. However, as the presence of these substances in water can be harmful for ecosystems and human health [4-7], and the inclusion of new quality criteria in water reuse regulations concerning this kind of pollution is expected shortly.

Most MPs are only efficiently degraded by hydroxyl radicals (HO·), which can be generated by Advanced Oxidation Processes (AOPs). Among these techniques, photo-Fenton process has demonstrated its efficiency in the removal of several organic compounds and pathogens [8-11]. Nevertheless, acidic conditions under which this treatment is effective make the process economically unattractive for full-scale application [12, 13]. To solve this inconvenience and work at natural pH, several chelating agents have been studied to keep iron complexed and avoid its precipitation at pH above 2.8 (i.e., the optimal working conditions for photo-Fenton process). Compounds such as EDTA (Ethylenedinitrilotetraacetic acid) and EDDS (Ethylenediamine-N, N'-disuccinic acid), as well as citric and oxalic acids have been the most investigated [14-17]. However, the low stability of the corresponding iron complexes eventually provokes the precipitation of iron during the treatment, consequently decreasing the removal efficiency of MPs. Recently, studies with other chelating agents such as DTPA (Diethylene triamine pentaacetic acid) and EDDHA (Ethylenediamine-*N*,*N′*-bis(2-hydroxyphenylacetic acid)) have also demonstrated their efficiency in abatement of organic micropollutants and bacterial inactivation [18, 19]. All of these iron chelates are approved by the European Commission for their agricultural use [20] as these can be applied in the form of ferric chelates to provide the crops with the iron required to produce chlorophyll and some enzymatic functions involved in respiration and metabolism. In this sense, an investigation on new organic fertilizers more sustainable with the environment studied the EDDS as a fertilizer to avoid the chlorosis in plants. The results revealed that EDDS is suitable for the correct development of the plants [21] and it is more biodegradable in soils than DTPA or EDTA, which are also commonly employed in agriculture as organic fertilizers.

Unlike the most common chelating agents, DTPA and EDDHA iron complexes present very high stability. Consequently, degradation rates of MPs are slow, although their use can involve advantages such as having a higher amount of chelated iron at the end of the treatment [18]. To improve the process, an equilibrium between iron availability and complexes stability in solution is needed to ensure a sustained production of hydroxyl radicals during the entire treatment and, consequently, a good treatment efficiency.

The aim of this work is to test the performance of different iron chelates in the treatment of secondary wastewater effluent by photo-Fenton, for their subsequent reutilization in agriculture. The selected endpoints for assessment of the treatment efficiency were the abatement of three representative micropollutants: acetamiprid (ACMP), propranolol (PROP) and sulfamethoxazole (SMX). For the first time, as far as we have been able to know, five different organic fertilizers (EDTA, EDDS, DTPA, EDDHA and HEDTA (2-Hydroxyethyl ethylenediamine-*N*,*N′*,*N′*-triacetic acid)) were compared in the same study under similar and feasible operational conditions, showing the potential applicability of each compound. Moreover, some of the best performing chelates were combined and tested in additional photo-Fenton experiment. The aim of this part was to explore possible performance increase of the process with the use of chelates mixtures, taking advantage of the particular properties of each compound concerning the ability of keeping iron complexed and available for catalytic reactions conducting to HO· generation. Apart from MPs abatement, BOD_5 after treatment was evaluated to compare the results of treated wastewater with the legislation for agricultural water reuse.

2. Material and methods

2.1. Chemicals

Propranolol hydrochloride (PROP), acetamiprid (ACMP), sulfamethoxazole (SMX), EDDS-Na solution and liver bovine catalase from bovine liver were acquired from Sigma-Aldrich. Organic fertilizers (bought with iron chelated) DTPA-Fe (7% of iron), EDTA-Fe (13.3% of iron) and HEDTA-Fe (13.0% of iron), used as iron chelates, were purchased from Phygenera, Germany. EDDHA-Fe (6.0% of iron) was obtained from Fertiberia. Acetonitrile, orthoposphoric acid, ferrous sulfate ($FeSO_4 \cdot 7H_2O$) hydrogen peroxide (H_2O_2, 30% w/v), o-Nitrobenzaldehyde (98%) and ethanol (96%, v/v) were acquired from Panreac Quimica.

2.2. WWTP effluent

Secondary effluent from a membrane bioreactor (MBR) of a wastewater treatment plant (WWTP) located in Barcelona, Spain (plant of Gavà-Viladecans; 384000 population equivalent (PE); DF (design flow): 64000 m^3 d^{-1}) was chosen to perform the experiments. The MBR is a combination of conventional activated sludge (CAS) and external membrane post-treatment by ultrafiltration. Table 1 lists the principal parameters of the WW.

Table 1. Physic-chemical parameters of wastewater.
N/A: below the detection level.

Parameters	**MBR**
pH	7.8
Turbidity (NTU)	0.3
UV_{254} (m^{-1})	19.1
TOC (mg C L^{-1})	7.0
DOC (mg C L^{-1})	6.7
Total alkalinity (mg $CaCO_3$ L^{-1})	233.2
HCO_3^- (mg HCO_3^- L^{-1})	279.8
Cl^{-1} (mg L^{-1})	591.6

SO_4^{2-} (mg L^{-1})	168.8
$N\text{-}NO_2^-$ (mg L^{-1})	0.4
$N\text{-}NO_3^-$ (mg L^{-1})	N/A
PO_4^{3-} (mg L^{-1})	N/A

2.3. Experimental procedure

All experiments were carried out in a solar simulator (Xenonterm-1500RF.CCI) with a Xenon lamp (1.5 kW) (wavelength range: 290-400 nm; irradiance: $6.6\cdot10^{-7}$ Einstein$\cdot L^{-1}$ s^{-1} (13.9 W m^{-2}) obtained by o-Nitrobenzaldehyde actinometry. The methodology to prepare the solutions to carry out the actinometry was extracted from De la Cruz et al. 2013 [22]. The emission spectrum can be found in figure S1 of supplementary information. The tubular photoreactor (25 cm length x 2 cm diameter) was located on the axis of a parabolic mirror made of reflective aluminum (*reflectivity between 0.8 and 0.9)*, at the bottom of solar simulator. The total volume of each experiment was 1L and the solution was continuously recirculated from the feeding tank (magnetically stirred) to the tubular photoreactor. The temperature was controlled by Haake C-40 bath and keep constant at 25ºC. More information about the experimental set-up can be found in figure 1.

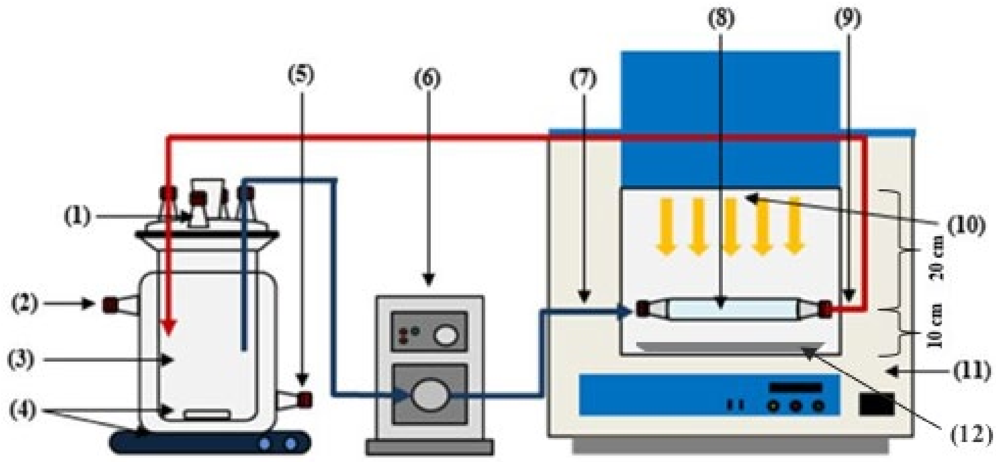

Figure 1. Experimental setup. (1) Sampling orifice; (2) Thermostatic bath-IN; (3) Feeding tank; (4) Magnetic stirrer; (5) Thermostatic bath-OUT; (6) Peristaltic pump; (7) Recirculation IN; (8) Tubular photoreactor; (9) Recirculation OUT; (10) Xenon lamp; (11) Solar simulator chamber; (12) Parabolic mirror.

To prepare the dissolutions with iron chelates, an appropriate amount of each organic fertilizer was added to WW. The concentration of each one was calculated according to the percentage of iron content (information in section 2.1) in order to obtain a concentration of 5 mg L^{-1} of iron in solution (which is the maximum concentration in irrigation water permitted by international regulations) [23, 24]. To perform the experiments with two iron chelates an appropriate amount of each organic fertilizer, according to the iron content of each one, was added to solution also to achieve a total concentration of 5 mg L^{-1} of iron. In the mixtures with EDDS, which was the only one that was not acquired as an iron chelate, a molar ratio of 1:1 (EDDS: Fe(II)) was selected based on previous studies [25]. In these cases, the EDDS was firstly added to the solution and then the iron, to ensure a good chelation. After this, the corresponding organic fertilizer was added to obtain the total iron concentration. A concentration of 0.25 mg L^{-1} of PROP, ACMP and SMX was spiked to the WW (total concentration of 0.75 mg L^{-1}). Finally, hydrogen peroxide (50 mg L^{-1}) was added just before the reaction began. Samples were retired periodically from the tank during 180 minutes and liver bovine catalase was employed to stop the reaction (10 µL of liver bovine catalase at a concentration of 200 mg L^{-1} to 5 mL of each sample). Samples to analyze the total iron content were filtered with 0.20 µm PVDF filter to ensure a good read of soluble (chelated and not) iron. In addition, ascorbic acid was added to the sample to have the total soluble iron.

The degradation of MPs was plotted considering the accumulated energy (Q_{acc}, kJ L^{-1}), which was calculated according to Eq.1 [22, 26].

$$Q_{acc} = \sum_{i=0}^{n} \frac{I \cdot \Delta t_i}{V} \qquad \text{(Eq.1)}$$

I is the irradiation entering the photoreactor (kJ s^{-1}), Δt_i is the increment of the time of reaction (s) and V is the reaction volume (L).

2.4. Analytical measurements

The concentration of MPs (PROP, ACMP and SMX) was followed by High Performance Liquid Chromatography (HPLC Infinity Series, Agilent Technologies), using a C-18 Tecknokroma column (250 x 4.6 mm i.d; 5µm particle size). Acetonitrile (20%) and water acidified with orthophosphoric acid (pH=3) (80%) were employed as mobile phases. The flowrate was 1 mL min^{-1} and the injection volume was set to 100 µL. Three wavelengths were fixed according to absorbance of each compound: 214, 250 and 270 nm for PROP, ACMP and SMX, respectively. Equal than MPs, the concentration of o-Nitrobenzaldehyde was measured by HPLC with the column aforementioned. The mobile phases were acetonitrile and water (pH=3) (60:40, respectively), UV detection was set to 258 nm and 0.6 mL min^{-1} was fixed as a flow rate. The monitoring of H_2O_2 and total iron in solution was performed by colorimetric method of metavanadate [27] and o-phenantroline procedure (ISO 6332), respectively. The BOD_5 was carried out using the 5210-standard method.

3. Results and discussion

3.1. Efficiency of organic fertilizers in photo-Fenton process

First of all, 3 new organic fertilizers (EDDHA, HEDTA and DTPA) and EDDS and EDTA, as a conventional fertilizers used in photo-Fenton, were tested and compared as iron chelates in the abatement of three MPs (PROP, ACMP, SMX) by photo-Fenton at natural pH. These MPs were selected, as model compounds, due to their different kinetic constants with hydroxyl radicals ($k_{PROP,HO} = 1.0 \cdot 10^{10}$ M^{-1} s^{-1} [28], $k_{SMX,HO} = 5.5 \cdot 10^{9}$ M^{-1} s^{-1} [29], $k_{ACMP,HO} = 2.1 \cdot 10^{9}$ M^{-1} s^{-1} [30]). Many research works are mainly focused on the use of one or two chelating agents [31-35]. However, to the best of our knowledge, in this study 5 chelating agents were tested and compared between them, for a first time. All experiments were carried out in real secondary WW (MBR) using 5 mg L^{-1} of iron and 50 mg L^{-1} of H_2O_2. The results are given in figure 2a, b and c (PROP, ACMP and SMX respectively). In addition, the photolysis of three MPs in MBR matrix was previously evaluated as a control test and the results at the end of the treatment (Q_{acc}= 2.31 kJ L^{-1}; 180 min) were 12.4, 5.3 and 2.4% of depletion for PROP, SMX and ACMP, respectively.

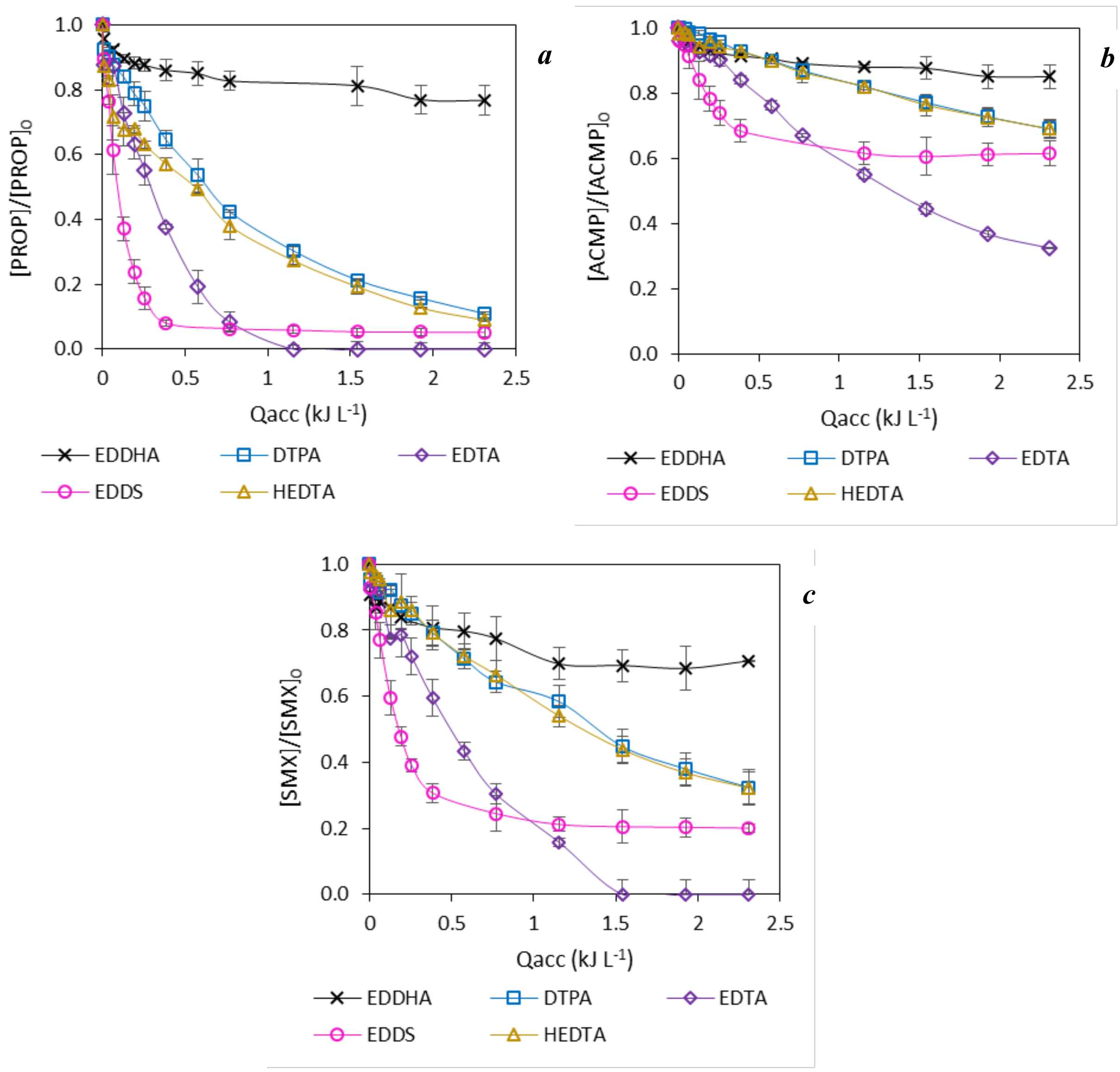

Figure 2. a) PROP b) ACMP and c) SMX degradation as a function of the accumulated energy for experiments with different organic fertilizers as chelating agents in photo-Fenton in MBR secondary effluent (pH= 7.8). $[PROP]_0$ = $[ACMP]_0$ = $[SMX]_0$ = 0.25 mg L^{-1}; $[Fe]_0$ = 5 mg L^{-1}; $[H_2O_2]_0$ = 50 mg L^{-1}. Total treatment time: 180 min, Qacc=2.31 kJ L^{-1}.

Among different micropollutants, PROP achieved the best degradations with the five chelating agents followed by SMX, while ACMP presented the lowest removals in all conditions. This fact is in accordance with the kinetic constant of each micropollutant with hydroxyl radicals, being PROP the highest and ACMP the lowest, as commented before.

Regarding the chelating agents, the best removals were achieved for EDTA (100% for PROP and SMX and 67.6 % for ACMP) and the worst degradations were presented for EDDHA (23.3, 29.3 and 15% for PROP, SMX and ACMP, respectively) at the end of the treatment (Q_{acc}= 2.31 kJ L^{-1}; 180 min). The removals of the MPs when using DTPA and HEDTA were very similar (89 and 91.1% for PROP, 67.6 and 67.8% for SMX and 31 % for ACMP, respectively). However, a distinct behavior was observed for EDDS. As can be seen in figures 2 a, b and c, the degradation of three MPs was faster until 0.39 kJ L^{-1} (30 minutes). Then, the removal dropped significantly, failing to reach the complete degradation. Results for EDDS at the end of the treatment (Q_{acc}= 2.31 kJ L^{-1}, 180 minutes) were 94.8, 79.9 and 38.5% for PROP, SMX and ACMP, respectively, close to the removals at 0.39 kJ L^{-1} (30 minutes), 89.9, 69.3 and 31.7% for PROP, SMX and ACMP, respectively.

Removal kinetics are closely linked to the release and subsequent precipitation of iron during the treatments. Figure 3 shows the evolution of total iron in solution along the performed photo-Fenton experiments. As it can be observed, faster MPs removal kinetics corresponds to EDDS which presented higher iron release and precipitation compared with the other chelating agents, already from the beginning of the experiment. On the contrary, EDDHA with the lower iron lost kinetics obtained the worse MPs removal. In the particular case of EDDS, after 30 minutes of reaction (0.39 kJ L^{-1}) and at the highest MPs removal kinetics, the available iron was still about 60% of the initial chelated iron that is about 3 mg L^{-1}. The abrupt efficiency removal drop from that point could be related with the generation of insoluble species of iron with by-products of the chelate agent and/or the organic matter present in the wastewater, degreasing the performance of the photo-Fenton reaction. Thus, soluble iron dropped to 25% (less than 1ppm of soluble iron) at 60 minutes of reaction (0.39 kJ L^{-1}) and it was almost completely precipitated by the end of the experiment.

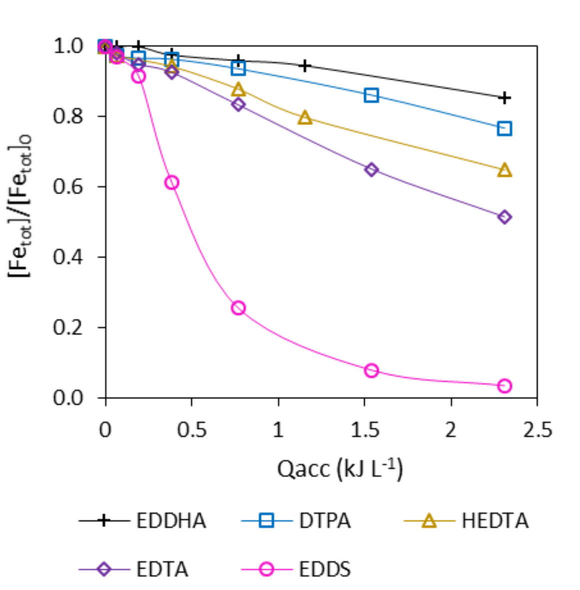

Figure 3. Evolution of total iron in solution as a function of the accumulated energy for experiments with different organic fertilizers as a chelating agents in photo-Fenton process of MBR secondary effluent. $[PROP]_0 = [ACMP]_0 = [SMX]_0 = 0.25$ mg L^{-1}; $[Fe]_0 = 5$ mg L^{-1}; $[H_2O_2]_0 = 50$ mg L^{-1}. Total treatment time: 180 min, Qacc=2.31 kJ L^{-1}.

MPs removal and iron availability are related to the stability constant (k_{stab}) of the complexes with iron (See Table 2). Among studied chelates, EDDS presents one of the lowest constants, which is in accordance with high iron precipitation during the experiment. No data were found for the stability constant of EDDS-Fe(II). However, it is expected that the constant with iron (II) would be lower than stability constant with iron (III), as it happens with other chelating agents (see Table 2). On the other hand, EDDHA and DTPA, which present high stability constants with iron, revealed low kinetic removal rates with the three MPs.

Table 2. Principal parameters of different chelating agents for their comparison. Total degradation of PROP and iron in solution were the values at the end of the treatment (2.31 kJ L^{-1}; 180 min). k_1 is the kinetic constant at initial time (0-0.39 kJ L^{-1}, 30 min) and k_2 is the kinetic from 30 min to 90% of PROP degradation. (1) Total degradation not reached 90%; (2) Total degradation at 0.39 kJ L^{-1}. Values of Kstab were retrieved from references [36-38].

	Total PROP removal (%)	k_1 (kJ^{-1})	R^2 (k_1)	k_2 (kJ^{-1})	R^2 (k_2)	Iron in solution (%)	K_{stab} (Ligand-Fe(III))	K_{stab} (Ligand-Fe(II))
EDTA	100	2.36	0.98	3.91	0.99	52.0	25.10	14.33
EDDS	94.8	6.21	0.98	0.21	0.83	4.0	22.0	-
HEDTA	91.1	1.00	0.81	0.90	0.99	64.9	19.80	12.20
DTPA	89.0	1.09	0.97	1.00	0.99	77.0	28.60	16.55
EDDHA	23.3	0.35	0.80	(1)	(1)	85.5	35.09	-
EDDS-EDTA	100	6.97	0.99	(2)	(2)	78.2	-	-
EDDS-DTPA	74.6	3.54	0.99	1.06	0.98	70.0	-	-
EDTA-DTPA	100	3.14	0.94	2.53	0.96	56.3	-	-

The stability constant of the chelates with iron is linked to their chemical structure, particularly the strength, functional groups, number of the chelates interactions and pH [18, 39]. Chemical structures of five complexes can be seen in Table 3.

Table 3. Properties of different iron complexes employed in this study.

Compound	**Molecular formula**	**Chemical structure**	**Molecular weight (g/mol)**
HEDTA-Fe	$C_{10}H_{18}FeN_2O_7 \cdot 5H_2O$	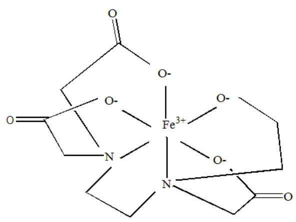	424.11

DTPA-Fe	$C_{14}H_{18}N_3O_{10}FeNa_2$	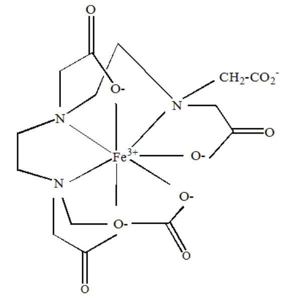	490.20
EDTA-Fe	$C_{10}H_{12}N_2O_8FeNa\cdot 3H_2O$	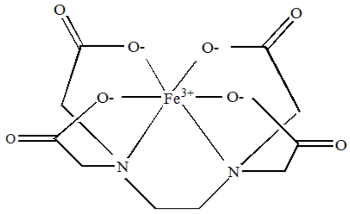	421.10
EDDHA-Fe	$C_{18}H_{16}N_2O_6FeNa$	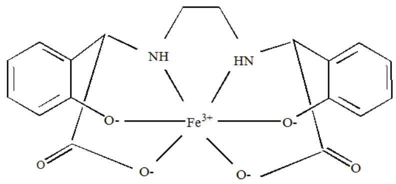	435.20
EDDS-Fe	$C_{10}H_9N_2FeNa_3O_8$	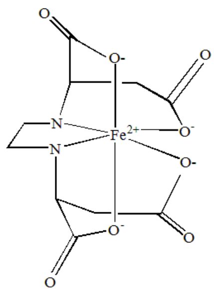	409.85

For EDDHA, the phenolate groups with hydroxyl in ortho position forming two bonds with iron (III) together with the octahedral geometry (coordination number = 6) give to the chelate greater stability [39]. In addition, the low MPs degradations could probably be related to the brown color of the iron complex, affecting light absorption capacity. In the case of DTPA, the complex presents a coordination number of 7 forming a pentagonal bipyramidal geometry which results in a higher stability than octahedral geometry. However, no phenolate groups in the structure makes overall DTPA stability lower than

EDDHA. These higher stabilities protect the iron from oxidants resulting in a lower iron leakage and lower MPs kinetic removal rates [39].

Different behavior was observed for HEDTA, which presents low stability constant, even lower than EDTA, but iron precipitation and MPs degradation were also significantly lower. Both chelates present octahedral geometry but EDTA presents 4 carboxylate groups while HEDTA only 3 (see table 3). Most probably EDTA complex undergoes higher photodegradation [39], increasing iron leakage and precipitation. In addition, the competition of Ca^{2+} and Zn^{2+} with Fe^{3+} for EDTA is increased at pH higher than 6.2 (secondary effluent pH=7.8), which would favor the iron precipitation [39]. DTPA also has 4 carboxylate groups but the additional coordination number, which implies a higher stability than HEDTA, balanced the photodegradation.

EDDS contains four carboxylate groups and the iron is not so structurally protected by the chelator from oxidants. Consequently, the iron can react more easily with H_2O_2, increasing hydroxyl radical kinetic generation, obtaining high MPs removal rates at initial times compared with the other complexes with higher stability constants. However, this lower iron protection by the chelator causes the rapid precipitation of iron, failing to reach the total degradation of MPs. According to obtained data presented in table 2, the kinetic rate (k_1) of PROP degradation by EDTA was 2.6 times lower than EDDS during the first 30 minutes of reaction, in accordance with the higher stability EDTA with iron. However, this high stability constant of EDTA allowed to keep more iron in solution after 30 minutes of the experiment and around 50% of iron remained in solution at the end of the treatment. Thus, photo-Fenton reactions can go further, achieving the total degradation in the case of PROP and SMX. In that case, the kinetic rate after 30 minutes of reaction (k_2) of EDTA was 18.6 times higher than EDDS. The same fact was observed between DTPA, HEDTA and EDDS. After 30 min, the kinetic rates (k_2) were 4.8 and 4.3 times higher for

HEDTA and DTPA than EDDS. More information about the kinetic rates can be found in figure S2 of supplementary material.

3.2. Organic fertilizers mixtures

The results explained in section 3.1 highlight the necessity to find the equilibrium between keeping the iron in solution and achieving high abatement rates for MPs. Mixtures of chelating agents with different stability with iron could be formulated towards this objective. In this section, EDDS, EDTA and DTPA were selected to perform the mixtures, according to the results of previous experiments. EDDS was included due to the high kinetic rates for MPs degradation at the beginning of the reaction and its good properties as a fertilizer in agriculture [21]. EDTA obtained total degradation of PROP and SMX and the best removal of ACMP. Finally, DTPA was chosen due to its high stability constant with iron, assuring the disposal of iron during all the experimentation, and its extended employment in agriculture compared with HEDTA. EDDHA was discarded due to the low degradations reached for three MPs. The mixtures assayed were EDDS-EDTA, EDDS-DTPA and EDTA-DTPA. Each combination was performed with 50% of the total iron content of each chelator achieving 5 mg L^{-1} of total dissolved iron. For comparison purposes, the experiments were carried out in the same MBR secondary effluent.

The Figures 4, 5 and 6 present the degradation curves of PROP, ACMP and SMX, in MBR matrix, using EDDS-EDTA, EDDS-DTPA and EDTA-DTPA mixtures, respectively.

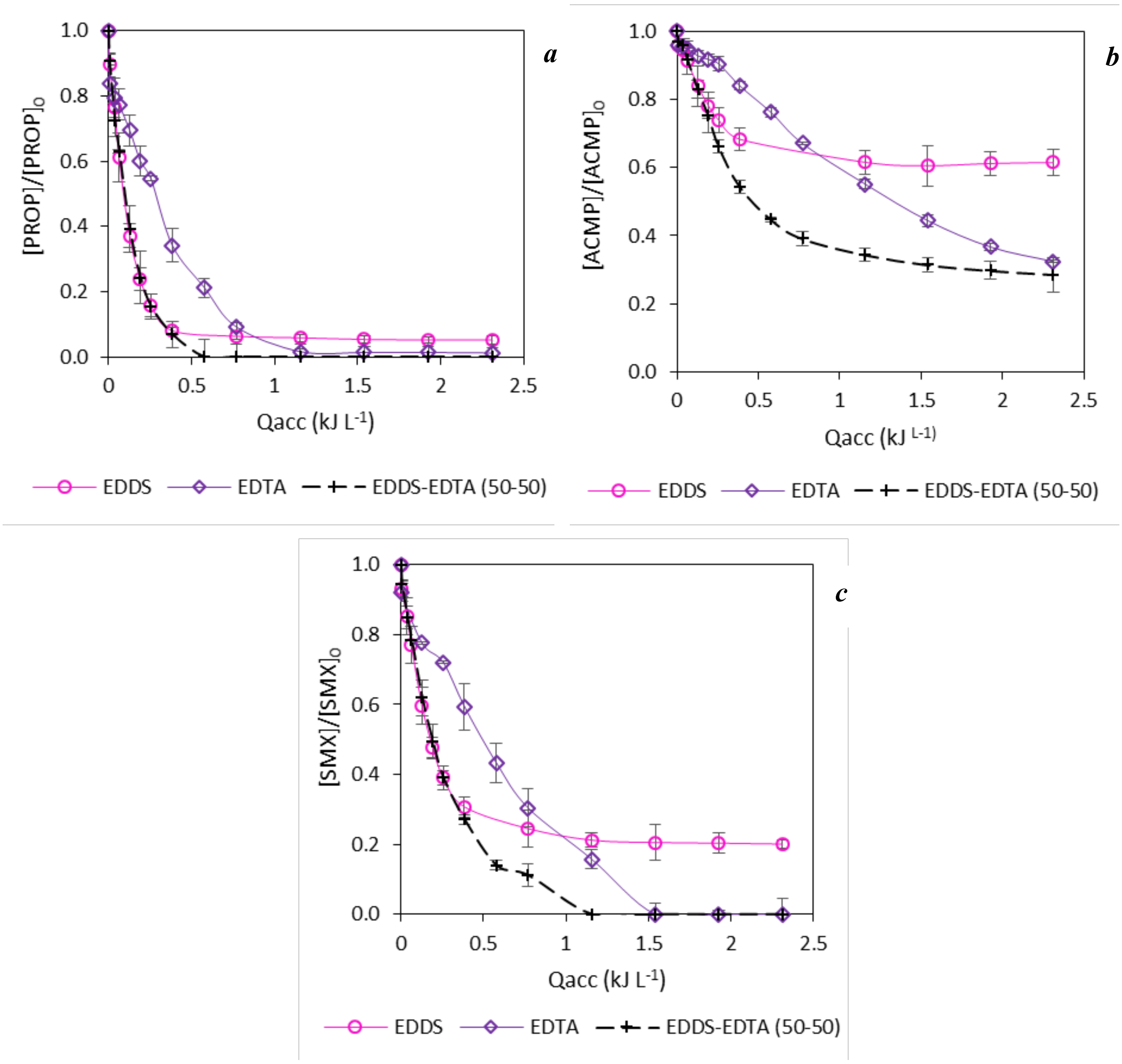

Figure 4. Profile of a) PROP b) ACMP and c) SMX degradation as a function of the accumulated energy for experiments with EDDS, EDTA and a mixture of both (50% EDDS + 50% EDTA) in photo-Fenton at natural pH in MBR secondary effluent. $[PROP]_0$= $[ACMP]_0$= $[SMX]_0$= 0.25 mg L^{-1}; $[Fe]_0$= 5 mg L^{-1}; $[H_2O_2]_0$= 50 mg L^{-1}. Total treatment time: 180 min, Qacc=2.31 kJ L^{-1}.

The mixture of EDDS and EDTA (Figure 4) showed the best results compared with the same chelates working alone since it maintained (see table 2 for kinetic of PROP and SMX) or even improved (ACMP) the high kinetic rate during the first minutes of the reaction. Moreover, the total degradation of PROP and SMX was reached in less irradiation time. For instance, total removal of PROP was achieved at 0.39 kJ L^{-1} (30 minutes) for the mixture EDDS-EDTA but at 1.16 kJ L^{-1} (90 minutes) for EDTA alone. This fact can be linked again with the evolution of total iron in solution, shown in Figure 7. The overall iron precipitation for the EDDS-EDTA mixture was slower than for EDDS alone. At 0.77 kJ L^{-1} (60 minutes), 50% of iron was in solution with the mixture of chelating agents, while in EDDS only 25% was keep in solution. At the end of the treatment, EDDS-EDTA mixture had 22% of the total iron in solution while EDDS only 4%. These results confirm that the chelates mixture EDDS-EDTA significantly improved the kinetics and the overall removals reached by the chelates used alone

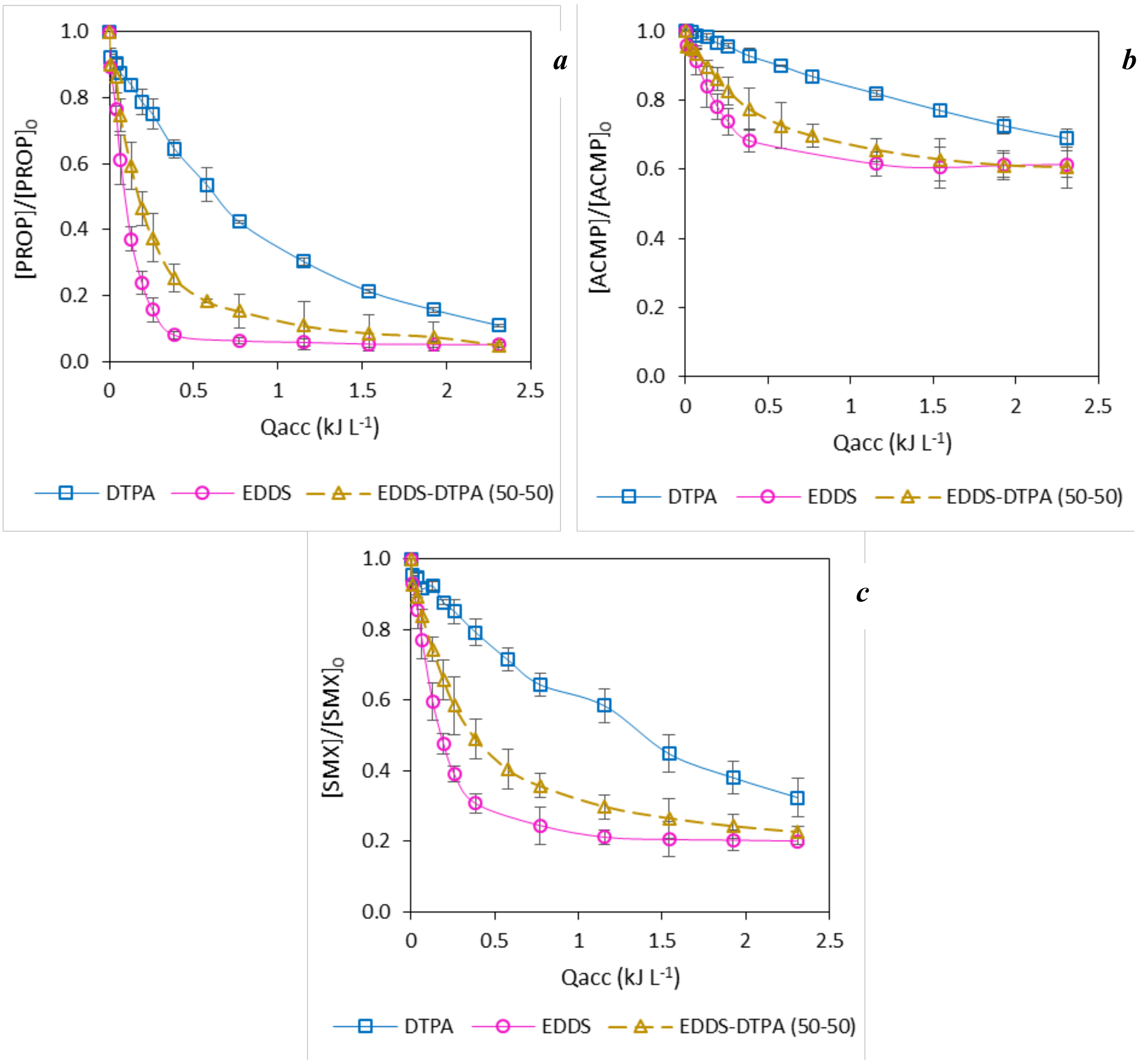

Figure 5. Profile of a) PROP b) ACMP and c) SMX degradation as a function of the accumulated energy for experiments with EDDS, DTPA and a mixture of both (50% EDDS + 50% DTPA) in photo-Fenton at natural pH in MBR secondary effluent. $[PROP]_0 = [ACMP]_0 = [SMX]_0 = 0.25$ mg L^{-1}; $[Fe]_0 = 5$ mg L^{-1}; $[H_2O_2]_0 = 50$ mg L^{-1}. Total treatment time: 180 min, Qacc=2.31 kJ L^{-1}.

Different results were obtained with the mixture EDDS-DTPA, as can be observed in Figure 5. MPs degradation kinetics was placed between the ones obtained with EDDS (higher) and DTPA (lower) alone. For example, at 0.39 kJ L^{-1} (30 minutes) the mixture obtained 75% of PROP removal, being a significant enhancement compared to DTPA (only 35.5 % of degradation), and little lower than the degradation obtained with EDDS. However, the iron remaining in solution was 86% for the combination EDDS-DTPA and only 61% for EDDS alone (see Figure 7). Thus, with the combination of the two chelating agents an equilibrium between high kinetic rates and a higher iron in solution disposal was achieved. In fact, at the end of experiment the level of MP degradation is practically the same.

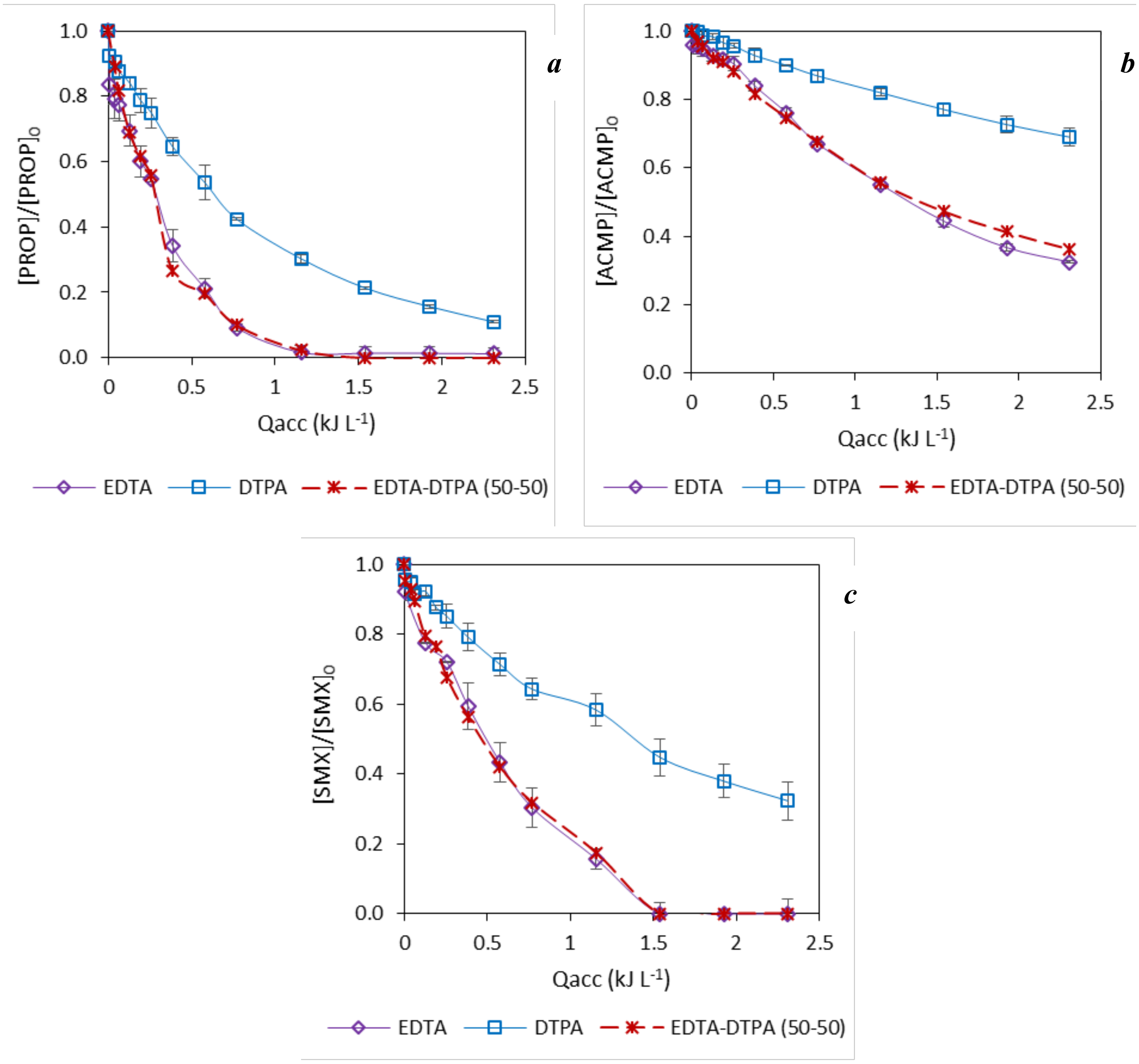

Figure 6. Profile of a) PROP b) ACMP and c) SMX degradation as a function of the accumulated energy for experiments with EDTA, DTPA and a mixture of both (50% EDTA + 50% DTPA) in photo-Fenton at natural pH in MBR secondary effluent. $[PROP]_0 = [ACMP]_0 = [SMX]_0 = 0.25$ mg L^{-1}; $[Fe]_0 = 5$ mg L^{-1}; $[H_2O_2]_0 = 50$ mg L^{-1}. Total treatment time: 180 min, Qacc=2.31 kJ L^{-1}.

When a combination of EDTA and DTPA was tested (Figure 6), the kinetic rate for the three MPs studied was very similar to the results with only EDTA. This fact is due to the kinetic rates for experiments with only one chelating agent (EDTA and DTPA) were more similar between them than experiments with only EDDS or DTPA (see Table 2). Thus, in Figure 6a an enhancement of PROP removal was observed (like Figure 5a) compared to experiment with only DTPA. With the combination EDTA-DTPA a 90% of PROP degradation was achieved at 0.77 kJ L^{-1} (60 minutes) equal than experiments with only EDTA. However, experiments with only DTPA reached 90% of PROP degradation at the end of the experiment (180 minutes, see Fig. 1) which implies a difference of 120 minutes more than the combination with EDTA. Although no kinetic rates and overall efficiency improvement was obtained, the EDTA-DTPA mixture retained higher iron content at the end of the photo-Fenton process, (75% of the initial value) compared with EDTA (about 50%). This fact represents an improvement since more soluble iron will arrive to the plants with the water effluent reuse to avoid ferric chlorosis.

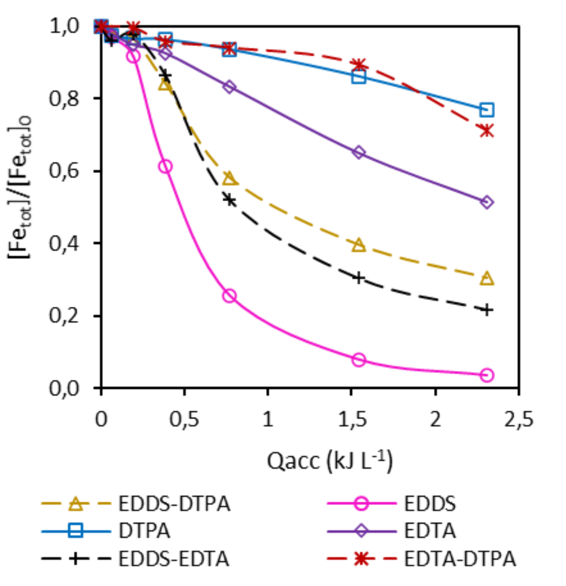

Figure 7. Evolution of total iron in solution as a function of the accumulated energy for experiments with different mixtures of chelating agents in photo-Fenton at natural pH in MBR secondary effluent. $[PROP]_0 = [ACMP]_0 = [SMX]_0 = 0.25$ mg L^{-1}; $[Fe]_0 = 5$ mg L^{-1}; $[H_2O_2]_0 = 50$ mg L^{-1}. Total treatment time: 180 min, Qacc=2.31 kJ L^{-1}.

3.3. Mixtures with different chelating agents' proportions

In order to optimize the combinations of chelating agents, mixtures using 25% of EDDS and 75% of EDTA or DTPA were also tested. These percentages would bring information about the proper combination of chelates to reach high removal rates, minimizing iron precipitation during the photo-Fenton treatment. Figure 8 shows the degradation curves of PROP, ACMP and SMX for the combination of 25% EDDS + 75% EDTA and the evolution of total iron in solution.

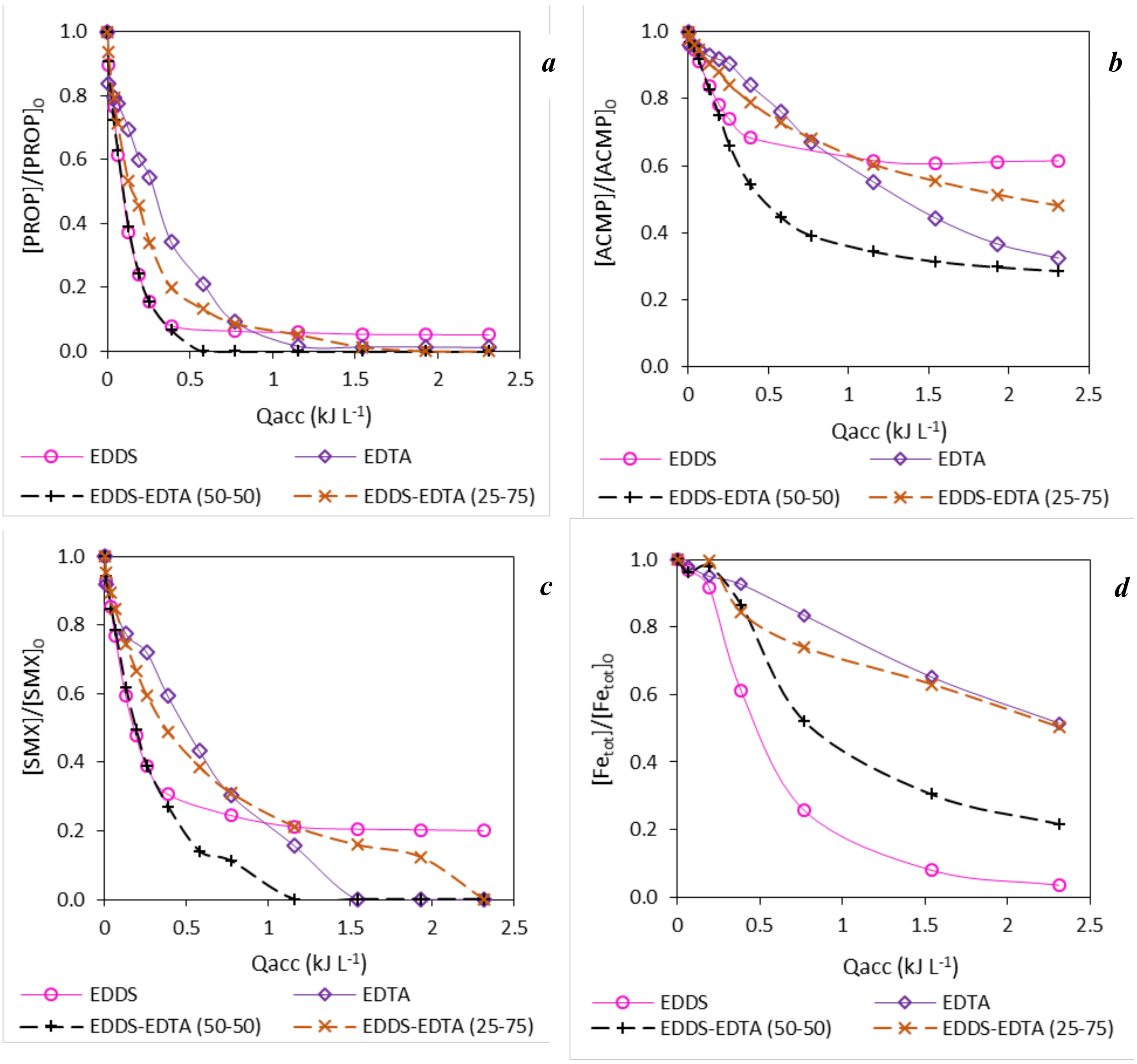

Figure 8. Profile of a) PROP b) ACMP and c) SMX degradation as a function of the accumulated energy for experiments with EDDS, EDTA and a mixture of both (25% EDDS + 75% EDTA) in photo-Fenton at natural pH in MBR secondary effluent. d) Evolution of total dissolved iron during different treatments. $[PROP]_0 = [ACMP]_0 = [SMX]_0 = 0.25$ mg L^{-1}; $[Fe]_0 = 5$ mg L^{-1}; $[H_2O_2]_0 = 50$ mg L^{-1}. Total treatment time: 180 min, Qacc=2.31 kJ L^{-1}.

As can see in figure 8, when a mixture of 25% EDDS and 75% of EDTA was performed the degradation curves for each MP are between the removal curves of two chelating agents tested alone until 0.77 kJ L^{-1} (60 minutes). Since this time, the degradation rate was lower than this one with EDTA alone but higher than the one obtained with EDDS alone. With the mixture 25% EDDS + 75% EDTA, a total degradation was achieved at 1.5 kJ L^{-1} (120 min) for PROP and at the end of the experiment for SMX (180 min). With 100% EDDS the complete degradation was not achieved for any micro-pollutant (see Fig. 8a, b and c). In the case of ACMP, a removal of 51.9% was reached with the mixture, at the end of the experiment, compared to only 38.5% achieved with EDDS alone. Moreover, iron evolution was similar to EDTA (see Fig. 8d), with 40% less of iron precipitation than experiments with 100% EDDS. These results are logical since 75% of iron is chelated with EDTA which present high stability constant. In that case, the tendency is closer to experiments with 100% EDTA than 100% EDDS compared with the combination of 50% EDDS + 50% EDTA, which was the other way around. In addition, the shape of the curves is also strongly related to the percentage of chelating agents. Thus 50% EDDS + 50% EDTA shows a degradation curve with a shape very similar to that of the EDDS alone. On the contrary, experiments with 25% EDDS + 75% EDTA show curves with a shape very close to this corresponding to EDTA alone. The same occurs with the experiments with 25% EDDS + 75% DTPA, where the degradation curves are very close to these ones corresponding to DTPA alone (see figure 9).

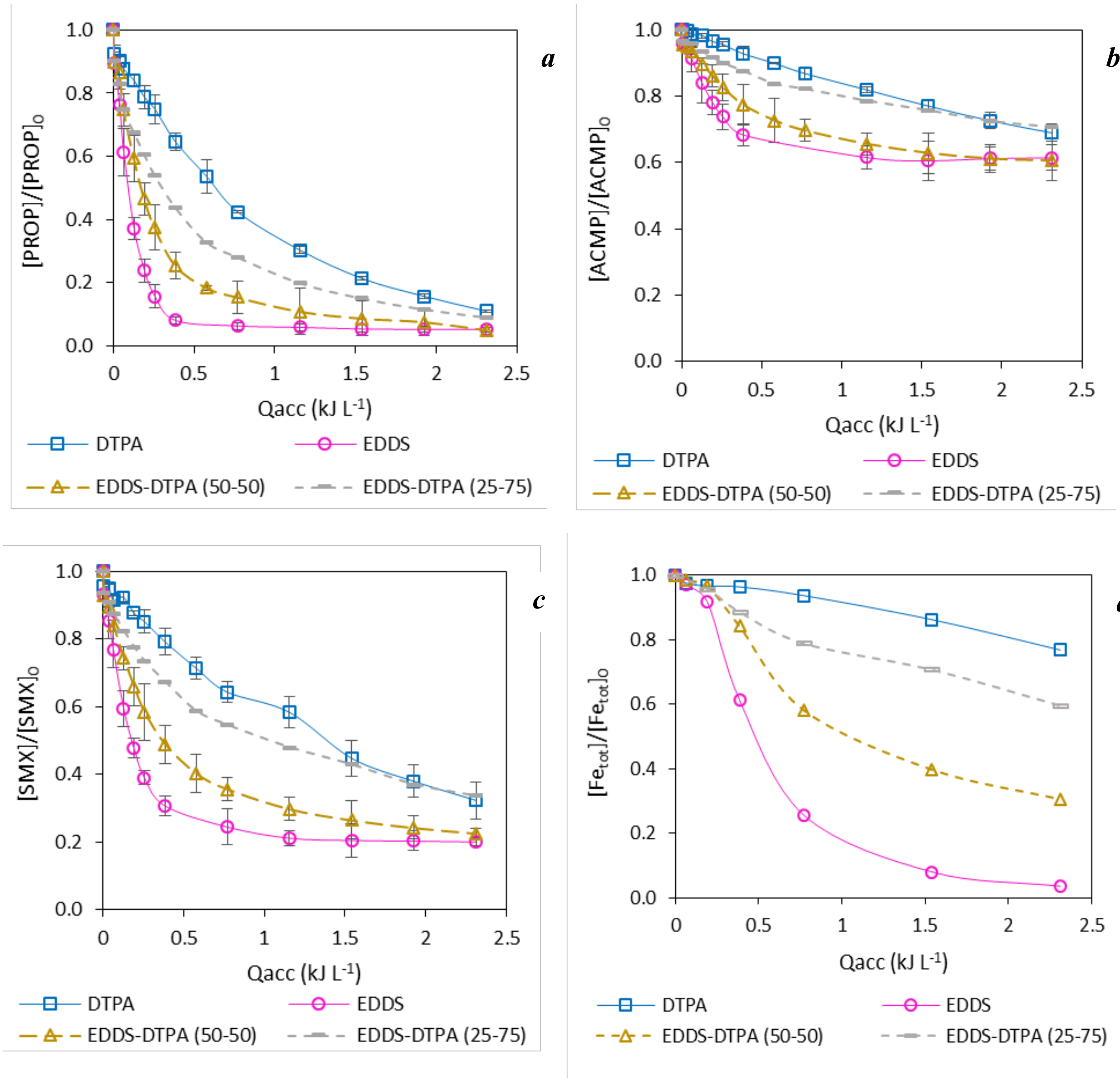

Figure 9. Degradation curves of a) PROP b) ACMP and c) SMX degradation as a function of the accumulated energy for experiments with EDDS, DTPA and a mixture of both (25% EDDS + 75% DTPA) in photo-Fenton at natural pH in MBR secondary effluent. d) Evolution of total dissolved iron during different treatments. $[PROP]_0 = [ACMP]_0 = [SMX]_0 = 0.25$ mg L^{-1}; $[Fe]_0 = 5$ mg L^{-1}; $[H_2O_2]_0 = 50$ mg L^{-1}. Total treatment time: 180 min, Qacc=2.31 kJ L^{-1}.

As can be observed in Fig. 9, the degradation lines for the two percentages tested for mixtures were between experiments with only EDDS and only DTPA. When 50%-50% combination was tested the tendency was more similar to EDDS. However, with 25% EDDS + 75% DTPA the trend was comparable to DTPA, as happened with EDDS-EDTA combination. Since the 50%-50% mixture presented this behavior it was reflected that EDDS had an important weight in the experiment.

The MPs removals obtained at the end of the treatment were only a little different for the two percentages tested. The results for 25% EDDS + 75% DTPA were: 90.9, 66.4 and 29.3% for PROP, SMX and ACMP, respectively. While the removals for 50% EDDS + 50% DTPA were: 95, 77.4 and 39.4% in the same order. It was observed that more close results were achieved for PROP. That fact is related to the highest kinetic rate with hydroxyl radicals for this compound. Although at the end of the treatment the different mixtures presented similar results, different kinetic rates were observed during the experiment. For instance, 74.6 and 56.2% were obtained for PROP with 50-50 and 25-75 at 30 minutes, respectively. That behavior was related to iron in solution and their availability. With 50%-50% more iron was chelated with EDDS which avoid higher kinetic rates at initial time. But, at the same time, the iron precipitation was higher than 25-75. That fact caused the degradation of MPs to slow down. Conversely, with 50-50 mixture the degradation was slower but steady. Thus, at the end of the treatment the difference of MPs degradation between two percentages of mixtures was lower than at first time of the experiment.

Comparing Fig. 8 and Fig. 9, different behavior was observed with the mixtures in both cases 50%-50% and 25%-75%. These differences are related to the stability constant of DTPA and EDTA. DTPA presents higher stability constant, making the reaction with peroxide more difficult. In the case of EDTA, the lower stability constant with iron and the medium stability constant of EDTA-Fe permits the faster degradation of MPs with the mixture performed with 50% EDDS + 50% EDTA. In addition, better MPs removals than only EDDS and close results than EDTA were achieved with 25% EDDS + 75% EDTA combination.

Moreover, the quantity of iron chelated is an important think to consider. If less iron is chelated the precipitation of this one will be slower (due to non-chelated iron remain in solution more time before to precipitate), being able to continue generating hydroxyl radicals. This fact influences on the mixtures using 50% EDDS + 50% EDTA, where 2.5 mg L^{-1} of iron is chelated with EDDS as long as the experiments with 100% of EDDS 5 mg L^{-1} of iron is chelated. Part of the yield increase is due to less iron precipitation with EDDS adding only 2.5 mg L^{-1} is chelated with EDTA, which maintain the iron chelated to produce more hydroxyl radicals. In the case of mixture 25%-75% only 1.25 mg L^{-1} is chelated with EDDS and 3.5 mg L^{-1} chelated with EDTA. More iron is chelated with a chelating agent which present high stability constant so that the kinetic rate is similar to this one. Otherwise, the iron precipitation will be slower but the quantity of iron chelated is also important in the photo-Fenton reactions. With only 1.25 mg L^{-1} of iron (25% EDDS) is not enough to achieve close kinetic than 5 mg L^{-1} (100% EDDS).

3.4. Biochemical Oxygen Demand at 5 days tests

The Proposal for a Regulation of the European Parliament and of the Council lists the minimum requirements for agricultural wastewater reuse [3] where BOD_5 (mgO_2 L^{-1}) is an important parameter to take into account. Figure 10 shows the values of BOD_5 after the photo-Fenton treatment with the chelates or mixture of chelates in MBR effluents. Process catalyzed by EDDS presented highest value of BOD_5 at the end of the treatment, reaching 19.6 mg O_2 L^{-1} while the combination of EDTA-DTPA achieved the lowest: 3.6 mgO_2 L^{-1}. The BOD_5 values of the treated effluent with combinations of 50% EDDS with EDTA or DTPA were placed between 13.6 and 9.6 mg O_2 L^{-1}, respectively. This fact represents an advantage compared to EDDS since the EU regulation for agricultural water reuse establishes four categories (A, B, C and D) depending on the quality of treated water. Category A fixes a value of $BOD_5 \leq 10$ mg O_2 L^{-1} and categories from B to D a level of $BOD_5 \leq 25$ mg O_2 L^{-1} [3]). Thus, when mixture of EDDS-DTPA was employed the treated effluent goes from category B to A (Table S1 and S2 in supplementary information explains different categories and quality requirements). Treated effluents using EDTA, DTPA and a mixture of EDTA-DTPA were also classified in category A.

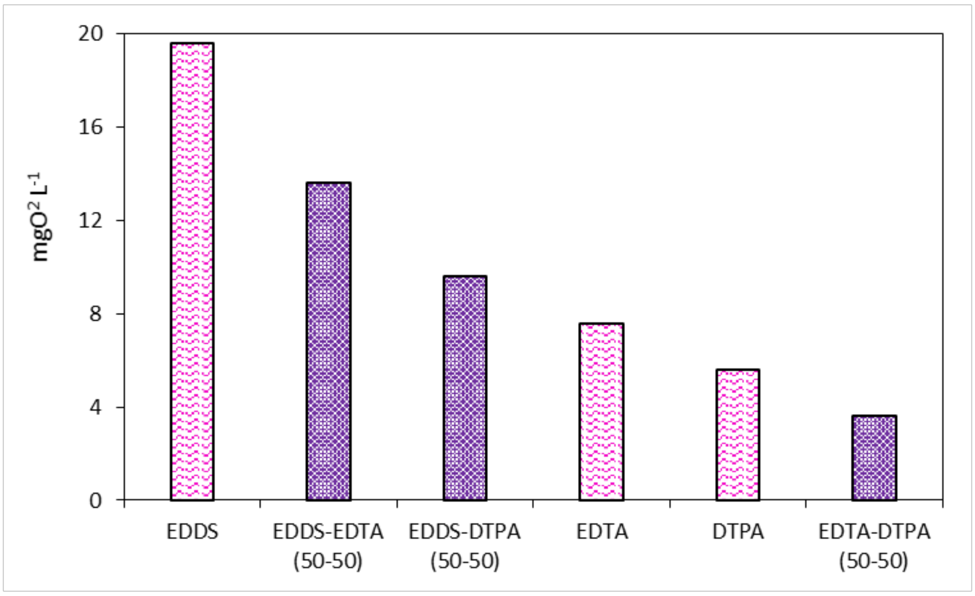

Figure 10. Biochemical Oxygen Demand at 5 days evaluation in MBR with photo-Fenton process at natural pH catalyzed by DTPA, EDTA, EDDS and three different combinations of these chelating agents at the end of the treatment. $[Fe]_0 = 5$ mg L^{-1}; $[H_2O_2]_0 = 50$ mg L^{-1}.

Finally, figure 11 was performed to obtain an overview of how the chelating agents and their mixtures respond to important parameters like MPs removal, iron stability, BOD_5 and chelating agent cost. The values of each parameter were normalized in the scale from 0 to 10, being the value of 10 the best conditions and 0 the worst. In supplementary material (Table S3) can be found the rules followed to normalize the different parameters.

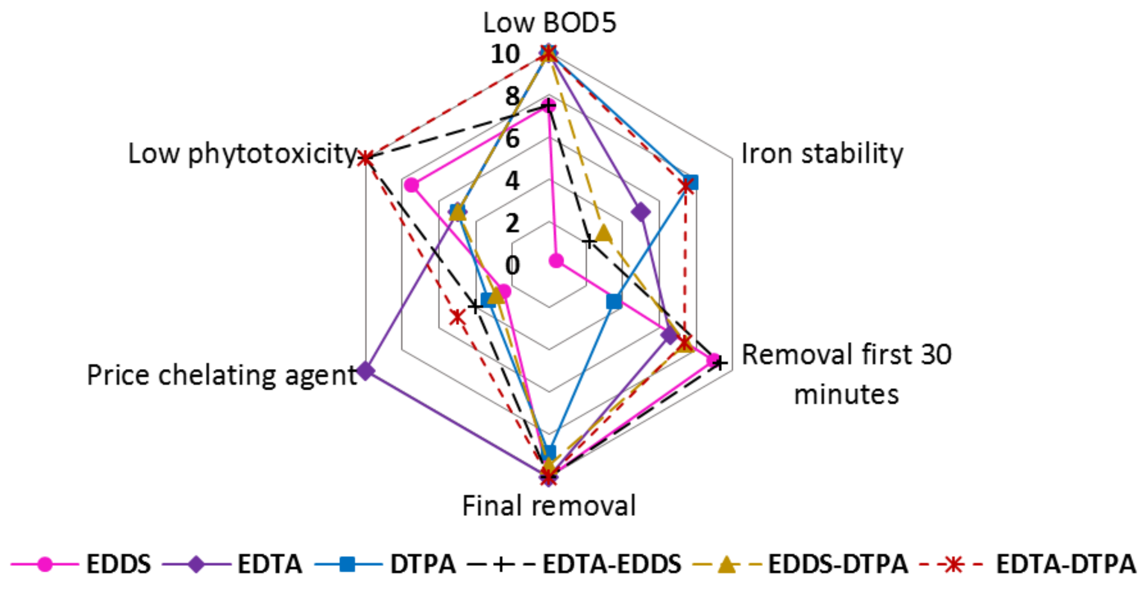

Figure 11. Overview of the response of different chelating agents and their mixtures for different parameters normalized from 0 to 10, being 10 the best conditions and 0 the worst.

As can been observed in figure 11, the experiments carried out with one chelating agent presented some deficiencies. For instance, EDDS show high price and low iron stability. EDTA presented medium iron stability. While DTPA displays high price and low removal at first 30 minutes. Nevertheless, with the combinations of these chelating agents an improvement was seen in all parameters. For example, the mixture composed by EDTA-DTPA (50%-50%) exhibited good enhancements in almost all parameters compared with single EDTA or DTPA. Only in the price was the second best under EDTA (price of mixture: 0.004€/experiment and 0.002 €/experiment for EDTA). In addition, the combination of EDTA-EDDS also reached good improvements in all parameters compared with EDDS: better removal at first 30 minutes and price (0.008 €/experiment for EDDS and 0.005 €/experiment for the mixture) were the enhancements more highlighted. Compared to EDTA, better removal at first 30 minutes was the improvement.

4. Conclusions

The organic fertilizers tested in this study were effective in removing the three selected micropollutants throughout photo-Fenton at natural pH. In the case of DTPA and HEDTA similar results were achieved in the MPs removal (about 90% for PROP, 70% for SMX and 30 % for ACMP) reaching worst results for ACMP because of its poor reactivity with hydroxyl radicals. EDDHA achieved the poor results (23.3, 29.3 and 15% for PROP, SMX and ACMP, respectively) due to its high stability constant with iron which affects its availability for Fenton reaction. EDTA and EDDS both presented good removals for PROP and SMX. However, only EDTA reached about 70% of ACMP. Removal kinetics and soluble iron availability resulted closely linked to the stability constant (k_{stab}) of the chelating agents. EDDS showed low stability constant with iron allowing high removal rates at initial times. However, the rapid iron precipitation decreased the overall efficiency of the process failing to reach total degradation for the three MPs. On the contrary, EDDHA with the highest stability constant showed the lower iron release and overall MPs removal efficiencies. Nevertheless, for the other 3 chelating agents studied with high stability constant, the iron precipitation was slower achieving less, but constant, hydroxyl radicals formation so that good MPs removals were observed at the end of the treatment.

For all this, assuring the process effectivity requires an equilibrium between to keep iron in solution and to achieve fast kinetic constants for MPs abatement. The three mixtures of different chelating agents tested (EDDS-EDTA, EDDS-DTPA and EDTA-DTPA, 50%-50%) show yields improvement. The EDDS-EDTA combination reached higher kinetic rates in the MPs abatement and final soluble iron availability, compared to the treatment using the chelates separately.

Tests of Biochemical Oxygen Demand at 5 days at the end of the treatment obtained that all effluents could reuse in agriculture according to current European legislation (Proposal for water reuse in agriculture [3]).

Finally, an evaluation of the most significant parameters of treated wastewater (low BOD_5, iron stability, MPs removal first 30 minutes, final MPs abatement and price of chelating agent) revealed that solar photo-Fenton using organic fertilizers can be applied in agriculture reuse of wastewater, being EDTA-EDDS mixture the most suitable among the chelating agents studied.

Acknowledgments

The authors wish to thank the Ministry of Economy and Competitiveness (project CTQ2017-86466-R, MINECO/FEDER, UE), AGAUR-Generalitat de Catalunya (project 2017SGR-131) and Nuria López FPU research fellowship (FPU-16/02101) financed by Ministry of Science, Innovation and Universities.

References

[1] E. Ortega-Gómez, B. Esteban García, M.M. Ballesteros Martín, P. Fernández Ibáñez, J.A. Sánchez Pérez, Inactivation of natural enteric bacteria in real municipal wastewater by solar photo-Fenton at natural pH, Water Research 63 (2014) 316-324.

[2] Food and Agriculture Organization of the United Nations. (2021). Land & Water: Water scarcity. Consulted at: http://www.fao.org/land-water/world-water-day-2021/water-scarcity/en/

[3] European Commission, Proposal for a Regulation of the European Parliament and of the Council of 28 May 2018 establishing the minimum requirements for water reuse, Official Journal of the European Communities 337 (2018) 1-27.

[4] N. De la Cruz, J. Giménez, S. Esplugas, D. Grandjean, L.F. de Alencastro, C. Pulgarin, Degradation of 32 emergent contaminants by UV and neutral photo-Fenton in domestic

wastewater effluent previously treated by activated sludge, Water Research 46 (2012) 1947–1957.

[5] D. Bertagna Silva, A. Cruz-Alcalde, C. Sans, J. Giménez, S. Esplugas, Performance and kinetic modelling of photolytic and photocatalytic ozonation for enhanced micropollutants removal in municipal wastewaters, Applied Catalysis B: Environmental 249 (2019) 211-217.

[6] N. López-Vinent, A. Cruz-Alcalde, L.E. Romero, M.E. Chávez, P. Marco, J. Giménez, S. Esplugas, Synergies, radiation and kinetics in photo-Fenton process with UVA-LEDs, Journal of Hazardous Materials 380 (2019) 120882.

[7] N. López, S. Plaza, A. Afkhami, P. Marco, J. Giménez, Treatment of diphenydramine with different AOPs including photo-Fenton at neutral pH, Chemical Engineering Journal 318 (2017) 112-120.

[8] I. Carra, J.A. Pérez Sánchez, S. Malato, O. Autin, B. Jefferson, P. Jarvis, Application of high intensity UVC-LED for the removal of acetamiprid with the photo-Fenton process, Chemical Engineering Journal 264 (2015) 690-696.

[9] Y. Aguas, M. Hincapie, P. Fernández-Ibáñez, M.I. Polo-López, Solar photocatalytic disinfection of agricultural pathogenic fungi (*Curvularia sp.*) in real urban wastewater, Science of the Total Environment 607-608 (2017) 1213-1224.

[10] A. Serra-Clusellas, L. De Angelis, C.H. Lin, P. Vo, M. Bayati, L. Sumner, Z. Lei, N.B. Amaral, L.M. Bertini, J. Mazza, L.R. Pizzio, J.D. Stripeikis, J.A. Rengifo-Herrera, M.M. Fidalgo de Cortalezzi, Abatement of 2,4-D by H_2O_2 solar photolysis and solar photo-Fenton-like process with minute Fe(III) concentrations, Water Research 144 (2018) 572-580.

[11] S. Miralles-Cuevas, D. Darowna, A. Wanag, S. Mozia, Malato S, I. Oller, Comparison of UV/H_2O_2, UV/$S_2O_8^{2-}$, solar/Fe(II)/H_2O_2 and solar/Fe(II)/$S_2O_8^{2-}$ at pilot

plant scale for the elimination of micro-contaminants in natural water, Chemical Engineering Journal 310 (2017) 514–524.

[12] I. De la Obra, L. Ponce-Robles, S. Miralles-Cuevas, I. Oller, S. Malato, J.A. Sánchez Pérez, Microcontaminant removal in secondary effluents by solar photo-Fenton at circumneutral pH in raceway pond reactors, Catalysis Today 287 (2017) 10–14.

[13] B. Esteban García, G. Rivas, S., J.A. Sánchez Pérez, Wild bacteria inactivation in WWTP secondary effluents by solar photo-Fenton at neutral pH in raceway pond reactors, Catalysis Today 313 (2018) 72-78.

[14] L. Clarizia, D. Russo, I. Di Somma, R. Marotta, R. Andreozzi, Homogeneous photo-Fenton processes at near neutral pH: A review, Applied Catalysis B: Environmental 209 (2017) 358-371.

[15] De Luca, A., Dantas, R.F., Esplugas, S., Study of Fe(III) -NTA chelates stability for applicability in photo-Fenton at neutral pH, Applied Catalysis B: Environmental 179 (2015) 372-379.

[16] I. García-Fernández, S. Miralles-Cuevas, I. Oller, S. Malato, P. Fernández-Ibáñez, M.I. Polo-López, Inactivation of *E. coli* and *E. faecalis* by solar photo-Fenton with EDDS complex at neutral pH in municipal wastewater effluents, Journal of Hazardous Materials 372 (2019) 85-93.

[17] S. Miralles-Cuevas, I. Oller, J.A. Sánchez Pérez, S. Malato, Removal of pharmaceuticals from MWTP effluent by nanofiltration and solar photo-Fenton using two different iron complexes at neutral pH, Water Research 64 (2014) 23-31.

[18] N. López-Vinent, A. Cruz-Alcalde, J.A. Malvestiti, P. Marco, J. Giménez, S. Esplugas, Organic fertilizer as a chelating agent in photo-Fenton at neutral pH with LEDs for agricultural wastewater reuse: Micropollutant abatement and bacterial inactivation, Chemical Engineering Journal 388 (2020) 124246.

[19] S. Nahim-Granados, I. Oller, S. Malato, J.A. Sánchez Pérez, M.I. Polo-López, Commercial fertilizer as effective iron chelate (Fe^{3+}-EDDHA) for wastewater disinfection under natural sunlight for reusing in irrigation, Applied Catalysis B: Environmental 253 (2019) 286-292.

[20] European Commission, Regulation (EC) No 2003/2003 of the European Parliament and of the Council of 13 October 2003 relating to fertilizers, Official Journal of the European Communities.

[21] S. López-Rayo, P. Nadal, J.J. Lucena, Novel chelating agents for iron, manganese, zinc and copper mixed fertilization in high pH soil-less cultures, Journal of the Science Food and Agriculture 96 (2016) 1111-1120.

[22] N. De la Cruz, V. Romero, R.F. Dantas, P. Marco, B. Bayarri, J. Giménez, S. Esplugas, O-Nitrobenzaldehyde actinometry in the presence of suspended TiO_2 for photocatalytic reactors, Catalysis Today 209 (2013) 209–214.

[23] Guidelines for Water Reuse 600/R-12/618; Environmental Protection Agency: Washington, DC, USA, 2012.

[24] R.S. Ayers, D.W. Westcot, Water Quality for Agriculture; Food and Agriculture Organization of the United Nations: Rome, Italy, 1985.

[25] N. López-Vinent, A. Cruz-Alcalde, C. Gutiérrez, P. Marco, J. Giménez, S. Esplugas, Micropollutant removal in WW by photo-Fenton (circumneutral and acid pH) with BLB and LED lamps, Chemical Engineering Journal 379 (2020) 122416.

[26] L.I. Doumic, P.M. Houre, M.C. Cassanello, M.A. Ayude, Mineralization and efficiency in the homogeneous Fenton Orange G oxidation, Applied Catalysis B: Environmental 142-143 (2013) 214–221.

[27] R.F. Pupo Nogueira, M.C. Oliveira, W.C. Paterlini, Simple and fast spectrophotometric determination of H_2O_2 in photo-Fenton reactions using metavanadate, Talanta 66 (2005) 86-89

[28] J. Benner, E. Salhi, T. Ternes, U. von Gunten, ozonation of reverse osmosis concentrate: kinetics and efficiency of beta blocker oxidation, Water Research 42 (2008) 3003-3012.

[29] M.M. Huber, S. Canonica, G.Y. Park, U. Von Gunten, Oxidation of pharmaceuticals during ozonation and advanced oxidation processes, Environmental Science and Technology 37 (2003) 1016–1024

[30] A. Cruz-Alcalde, C. Sans, S. Esplugas, Priority pesticides abatement by advanced oxidation water technologies: The case of acetamiprid removal by ozonation, Science of the Total Environment 599-600 (2017) 1454-1461.

[31] S. Arzate, M.C. Campos-Mañas, S. Miralles-Cuevas, A. Agüera, J.L. García Sánchez, J.A. Sánchez Pérez, Removal of contaminants of emerging concern by continuous flow solar photo-Fenton process at neutral pH in open reactors, Journal of Environmental Management 261 (2020) 110265.

[32] S. Miralles-Cuevas, F. Audino, I. Oller, R. Sánchez-Moreno, J.A. Sánchez Pérez, S. Malato, Pharmaceuticals removal from natural water by nanofiltration combined with advanced tertiary treatments (solar photo-Fenton, photo-Fenton-like Fe(II)-EDDS complex and ozonation), Separation and Purification Technology 122 (2014) 515-522.

[33] P. Soriano-Molina, S. Miralles-Cuevas, B. Esteban-García, P. Plaza-Bolaños, J.A. Sánchez Pérez, Two strategies of solar photo-Fenton at neutral pH for the simultaneous disinfection and removal contaminants of emerging concern. Comparative assessment in raceway pond reactors, Catalysis Today, article in press.

[34] K. Davididou, E. Chatzisymeon, L.Pérez-Estrada, I. Oller, S. Malato, Photo-Fenton treatment of saccharin in a solar pilot compound parabolic collector: Use of olive mill wastewater as iron chelating agent, preliminary results, Journal of Hazardous Materials 372 (2019) 137-144.

[35] A. De Luca, R.F. Dantas, S. Esplugas, Study of Fe(III)-NTA chelates stability for applicability in photo-Fenton at neutral pH, Applied Catalysis B: Environmental 179 (2015) 372-379.

[36] Dojindo Molecular Technologies, Inc, Table of Stability Constants, (2020). https://www.dojindo.com/images/Product%20Photo/Chelate_Table_of_Stability_Constants.pdf (accessed March 24, 2020).

[37] Martell, A.E., Motekaitis, R.J., Chen, D., Hancock, R.D., McManus, D., Selection of new Fe(III)/Fe(II) chelating agents as catalysts for the oxidation of hydrogen sulphide to sulfur by air, Canadian Journal of Chemistry 74 (1996) 1872-1879.

[38] Sierra, M.A., Gómez-Gallego, M., Alcázar, R., Lucena, J.J., Yunta, F., García-Marco, S., Effect of the tether on the Mg(II), Ca(II), Cu(II) and Fe(II) stability constants and pM values of chelating agents related to EDDHA, Dalton Transactions 21 (2004) 3741-3747.

[39] Sánchez, A. (2002). Mejora de la eficacia de los quelatos de hierro sintéticos a través de sustancias húmicas y aminoácidos (Tesis Doctoral). Universidad de Alicante, España.